

DIFFERENCE IN COLOR PROFILES BETWEEN LOWER AND UPPER CLASS GALAXIES: EVIDENCE FOR OUTSIDE-IN QUENCHING

HUI HONG^{1,2}, HUIYUAN WANG^{1,2}, H.J. Mo³

Draft version October 27, 2023

ABSTRACT

Subject headings: galaxies: halos - galaxies: general – methods: observational - methods: statistical

1. INTRODUCTION

Galaxy star formation quenching is important since redshift four.....

In the literature, many mechanisms are proposed to explain these correlations. For example, among environmental processes, ram pressure stripping, tidal stripping, strangulation and galaxy interaction. And among internal processes, such as stellar/supernova feedback, AGN feedback and morphological quenching... The two types of processes work together to shape the star formation of galaxies and the complex correlations with various internal and environmental factors, such as ???.

It is usually believed that in central galaxies, galaxy quenching is dominated by internal processes, while for satellites, internal and environmental quenching both work. Therefore, environmental processes are important for the star formation quenching in satellites.

Then describe these processes and their potential effect in details for ram pressure stripping. Here, it means the stripping of cold gas in galaxies by ram pressure. ram pressure may sometimes enhance the star formation rate via compressing gas.

for tidal stripping and galaxy interaction. Here it means the stripping of cold gas by tidal force. Galaxy interaction is very complicated, including mergers, harassment and other minor interaction. It also possibly induces AGN activity and thus AGN feedback, so it may also affect central galaxies.

for strangulation, ram pressure, tidal stripping and halo quenching may remove the hot gas of satellites.

Internal processes also work in satellites, to investigate these environmental processes, one often-used method is to compare centrals and satellites. For example, ??????. Here we show briefly the previous studies and their results, the correlations with different environmental factors.

However, it is still not clear which mechanisms play important roles for satellite quenching. One possible reason is that the strength of most of these mechanisms depend on both halo mass and halo-centric distance. And nature and nurture problem. And mention the underlying assumption for the comparison study. Another problem is that central may be also affected by environmental processes, i.e. internal and environmental processes are

entangled.

It is important to include more information, in particular the spatial resolved galaxy properties, and well designed comparison.

In this study, we ??????

see paper written by Weinmann et al. 2009. It seems that they compare the color profiles of satellites with centrals.

2. DATA AND METHODS

2.1. Galaxy sample

Here, we present the sample selection, and the methods in the literature to derive the basic parameters for galaxies, such as stellar mass, star formation rate, color, and B/T mass ratio. And we also briefly describe the methods to identify galaxy groups, classify central/satellite and assign halo mass.

Our sample is selected from the New York University Value Added Galaxy Catalog (NYU-VAGC; Blanton et al. 2005b) based on Sloan Digital Sky Survey Data Release 7 (SDSS DR7; Abazajian et al. 2009). We use the group catalog (Yang et al. 2007) thus the galaxies selected has the redshift range between 0.01 and 0.2, the spectroscopic completeness (C) greater than 0.7 and the r -band flux limit of $r = 17.72$ mag. The group catalog is constructed by the halo-based group-finding algorithm which is iterative and based on an adaptive filter modeled after the general properties of dark matter haloes.(Yang et al. 2005). The group catalog provides us with these parameters: stellar mass (M_*), $^{0.1}(g - r)$ color, halo mass, halo radius (r_{180}), most massive galaxy of each group. Stellar masses are computed by the stellar mass-to-light ratio and $(g - r)$ color from Bell et al. 2003 and the Kroupa initial mass function (IMF) adopted (Kroupa & Weidner 2003). $^{0.1}(g - r)$ colors are the g -band absolute magnitudes minus those of r -band in the AB magnitude system which are K corrected to $z = 0.1$ (Blanton & Roweis 2007). Halo masses are estimated from the total stellar mass of galaxies with $^{0.1}M_r - 5 \log h \leq -19.5$ for each group (Yang et al. 2007). Halo radii are calculated used the equation(5) of Yang et al. 2007. The halo-centric distance (r/r_{180}) of each galaxy are defined by the ratio of r to r_{180} where r is the projected distance between the galaxy and the luminosity-weighted center of its group. We adopt the most massive galaxy of a group as central galaxy while others are satellite galaxies.

We cross match the group catalog with the MPA-JHU catalog to obtain star formation rate (SFR) and 4000 Å break ($D_n(4000)$). The SFRs are computed using the method described in Brinchmann et al. 2004 and

¹ Key Laboratory for Research in Galaxies and Cosmology, Department of Astronomy, University of Science and Technology of China, Hefei, Anhui 230026, China

² School of Astronomy and Space Science, University of Science and Technology of China, Hefei 230026, China

³ Department of Astronomy, University of Massachusetts, Amherst MA 01003-9305, USA

the Kroupa IMF adopted (Kroupa & Weidner 2003). $D_n(4000)$ is used the Balogh et al. 1999 definition the ratio of the flux between the red and blue continua at 4000 Å. We also cross match with the bulge+disk decomposition catalog (Mendel et al. 2013). The B/T_m of a galaxy is calculated by the ratio of the bulge mass to the total stellar mass.

Since the main results of this article are on the basis of the radial profiles, we retrieve data from the SDSS CasJobs website (Stoughton et al. 2002) which include profMean azimuthally averaged radial surface brightness profiles in $g-$ and $r-$ band, petroR50 the radii containing 50% of $r-$ band Petrosian flux (R_{50} , in arcsec) and extinction the galactic extinctions (A_λ). The galaxy radial profile can be fitted by the Sérsic profile (Sersic 1968):

$$I(r) = A \exp[-(r/r_0)^{1/n}]. \quad (1)$$

The NYU-VAGC catalog provides one-component Sérsic fits (the model profiles) of the profMean (the observed profiles) above in which the seeing effect is taken into account (see the Appendix of Blanton et al. 2005a). The best fit to the variables: A , r_0 and Sérsic index n are fitted for $g-$ and $r-$ band separately. We also use the K-corrections performed with the kcorrect product version v4.1.4 to correct our magnitudes to $z = 0.1$.

2.2. Sample division

Here, we describe our thoughts about the comparison studies, and suggest that it is important to separate transition galaxies from the whole galaxy population. **Here, we show the SFR- M_* diagram and the demarcation lines used to separate star forming, transition and quiescent galaxy populations.** We also briefly discuss that the results do not change if we choose different the demarcation lines.

We also divide galaxies into different classifications, centrals (Cen), upper class satellites (UCS) and lower class satellites (LCS).

We also divide galaxies into different stellar mass and B/T bins.

listing the number of different types of galaxies in a table.

2.3. Cross matching Methods

We show our cross-match methods. show the match rate.

2.4. magnitude, color, mass and difference profiles

In this subsection, we show how the $g-$ and $r-$ band magnitude profiles are derived in the literature. We also present the model fitting to the magnitude profiles for all galaxies, in which the PSF effect is taken into account. So now we have two kinds of magnitude profiles. One is directly from the observational data, the other is the model fitting result as supplement. Then describe the method for evolution correction (to $z = 0.1$).

We then briefly describe the method to calculate the mass surface density profiles.

All color are $K + E$ corrected.

3. RESULTS

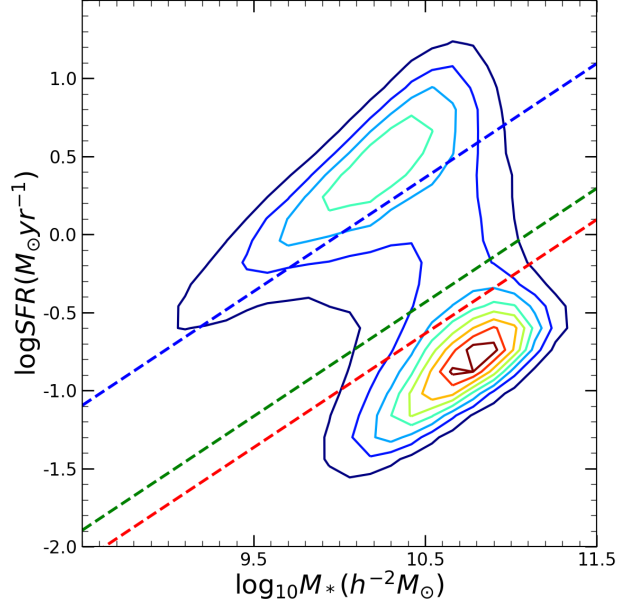


FIG. 1.— SFR as a function of stellar mass. The demarcation lines: $\log_{10}\text{SFR}=0.73\log_{10}M_*(h^{-2}\text{M}_\odot)-1.46\log_{10}h+A$, $A_{blue}=7.5$, $A_{green}=-8.3$, $A_{red}=-8.5$. Galaxies above the blue dashed line are divided into star-forming galaxies, between the blue and the red dashed lines are transition galaxies and below the red one are quiescent galaxies. Colors from blue to red of the contours correspond to the increasing contour levels. Here galaxies are not weighted.

We should compare lower class satellites and upper class satellites with centrals, separately. It may give us a clear picture on how environmental mechanisms work on satellites and whether the environmental efficiency depends on satellite mass.

we may remove the results for samples with less than 100 galaxies. We can show the model-fitting results as the primary results and present the results directly derived from observational data in the appendix. It might be better.

One problem is that our studies based on color, but we separate galaxies into blue cloud, green valley and red sequence galaxies by using SFR. In the appendix, we can show the major results, the color difference by using mass-color diagram to separate galaxies into three parts.

The location of these transition galaxies within the halos may tell us the condition for the underlying physical processes to work. It is still not clear how to show the results.

3.1. Statistics

we can define C1,C2, U1, U2, L1, L2 and L3 components in the stellar mass-color diagram. Then we show the probability distributions of D4000 and SSFR for these components. According to my analysis, C1, U1 and L1 are similar, C2 and U2 are similar and L2 is not far from them, L3 may be very different from L2 in both D4000 and SSFR, hinting that it is not the traditional quiescent galaxies. It is likely close to green valley galaxies. We should compare L3 component with the central and UCS galaxies in the same stellar mass and color ranges.

here, we can show more results. For example the stellar mass-color diagram for different subsamples.

We may also show the color- M_* diagram for various subsamples. We may also show the color- M_* diagram in different halos—actually, lower and upper class satellites of the same stellar mass reside in different halos.

the colors used in different figures should be defined in the same way.

The first figure have three panels. The left one shows the $(g-r)^{0.1}-M_*$ diagram for all galaxies with demarcation line from van den Bosch, which is used to separate star forming and quiescent galaxies, and the two lines that you used to define the green valley galaxies. Please show the formula for the three lines. The middle panel shows the $(g-r)^{0.1}-M_*$ diagram for the upper class galaxies, and the right panel shows the $(g-r)^{0.1}-M_*$ diagram for the lower class galaxies. All of these values are calculated with weight.

3.2. Comparison of satellites with centrals

The second figure has three panels. The figure shows the quenched fraction of galaxies (f_Q) as a function of M_h and M_* . The quenched fraction is defined as the fraction of galaxies that is quenched. Please calculate the quenched fraction with weight. The three panels show the results for galaxies with $0 \leq B/T_m < 1/3$, $1/3 \leq B/T_m < 2/3$ and $2/3 \leq B/T_m \leq 1$. Please also show the demarcation line that is used to separate upper class and lower class galaxies.

The third figure has 12 panels, 4 columns and 3 rows. In this figure, we show $(g-r)(R/R_e)-M_*$. The first row shows the upper class galaxies, the second row shows upper class satellites and the third row shows the lower class galaxies. The columns show the results with $R/R_e \leq 0.5$, $0.5 < R/R_e \leq 1.0$, $1.0 < R/R_e \leq 1.5$ and

$$1.5 < R/R_e \leq 2.0.$$

The fourth figure has 9 panels, 3 columns and 3 rows. This figure shows the median $(g-r)$ as a function of R/R_e with shadow showing the scatter for galaxies of $8.5 < \log M_*/h^{-1}M_\odot < 9$. The first column shows the results for blue cloud galaxies, the second column for green valley galaxies and the third column for red sequence galaxies. While the three rows are for $0 \leq B/T_m < 1/3$, $1/3 \leq B/T_m < 2/3$ and $2/3 \leq B/T_m \leq 1$, respectively. In each panel, you show the results for lower class galaxies, upper class galaxies (centrals and satellites together) and upper class satellites. For the upper class satellites, we do not show the scatter. **Note that the arrangement is different from what you showed before!!**

The fifth figure is similar to the fourth one, but for $9.5 < \log M_*/h^{-1}M_\odot < 10$.

The sixth figure is similar to the fourth one, but for $10.5 < \log M_*/h^{-1}M_\odot < 11$.

The 7th figure show the color difference as a function of R/R_e . 9 panels, 3 columns and 3 rows. The first column shows the results for blue cloud galaxies, the second column for green valley galaxies and the third column for red sequence galaxies. While the three rows are for $0 \leq B/T_m < 1/3$, $1/3 \leq B/T_m < 2/3$ and $2/3 \leq B/T_m \leq 1$, respectively.

4. SUMMARY AND CONCLUSION ACKNOWLEDGMENTS

This work is supported by the National Key R&D Program of China (grant No. 2018YFA0404503), the National Natural Science Foundation of China (NSFC, Nos. 11733004, 11890693, and 11421303), and the Fundamental Research Funds for the Central Universities. The work is also supported by the Supercomputer Center of University of Science and Technology of China.

REFERENCES

- Abazajian, K. N., Adelman-McCarthy, J. K., Agüeros, M. A., et al. 2009, The Astrophysical Journal Supplement Series, 182, 543
- Balogh, M. L., Morris, S. L., Yee, H. K. C., Carlberg, R. G., & Ellingson, E. 1999, The Astrophysical Journal, 527, 54
- Bell, E. F., McIntosh, D. H., Katz, N., & Weinberg, M. D. 2003, The Astrophysical Journal Supplement Series, 149, 289
- Blanton, M. R., Eisenstein, D., Hogg, D. W., Schlegel, D. J., & Brinkmann, J. 2005a, The Astrophysical Journal, 629, 143
- Blanton, M. R., & Roweis, S. 2007, The Astronomical Journal, 133, 734
- Blanton, M. R., Schlegel, D. J., Strauss, M. A., et al. 2005b, The Astronomical Journal, 129, 2562
- Brinchmann, J., Charlot, S., White, S. D. M., et al. 2004, Monthly Notices of the Royal Astronomical Society, 351, 1151
- Kroupa, P., & Weidner, C. 2003, The Astrophysical Journal, 598, 1076
- Mendel, J. T., Simard, L., Palmer, M., Ellison, S. L., & Patton, D. R. 2013, The Astrophysical Journal Supplement Series, 210, 3
- Sersic, J. L. 1968, Atlas de Galaxias Australes
- Stoughton, C., Lupton, R. H., Bernardi, M., et al. 2002, The Astronomical Journal, 123, 485
- Yang, X., Mo, H. J., van den Bosch, F. C., & Jing, Y. P. 2005, Monthly Notices of the Royal Astronomical Society, 356, 1293
- Yang, X., Mo, H. J., van den Bosch, F. C., et al. 2007, The Astrophysical Journal, 671, 153

APPENDIX

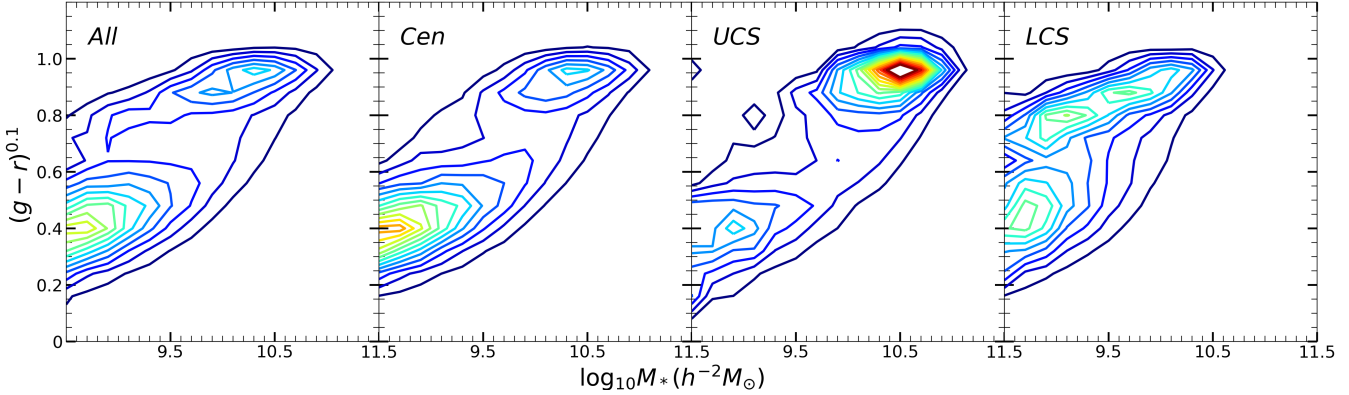


FIG. 2.— Panels from left to right are the $(g - r)^{0.1}$ - M_* diagrams of all galaxies, Cen (central galaxies), UCS (upper class satellite galaxies) and LCS (lower class satellite galaxies). Colors from blue to red correspond to increasing contour level. Each galaxy is weighted here.

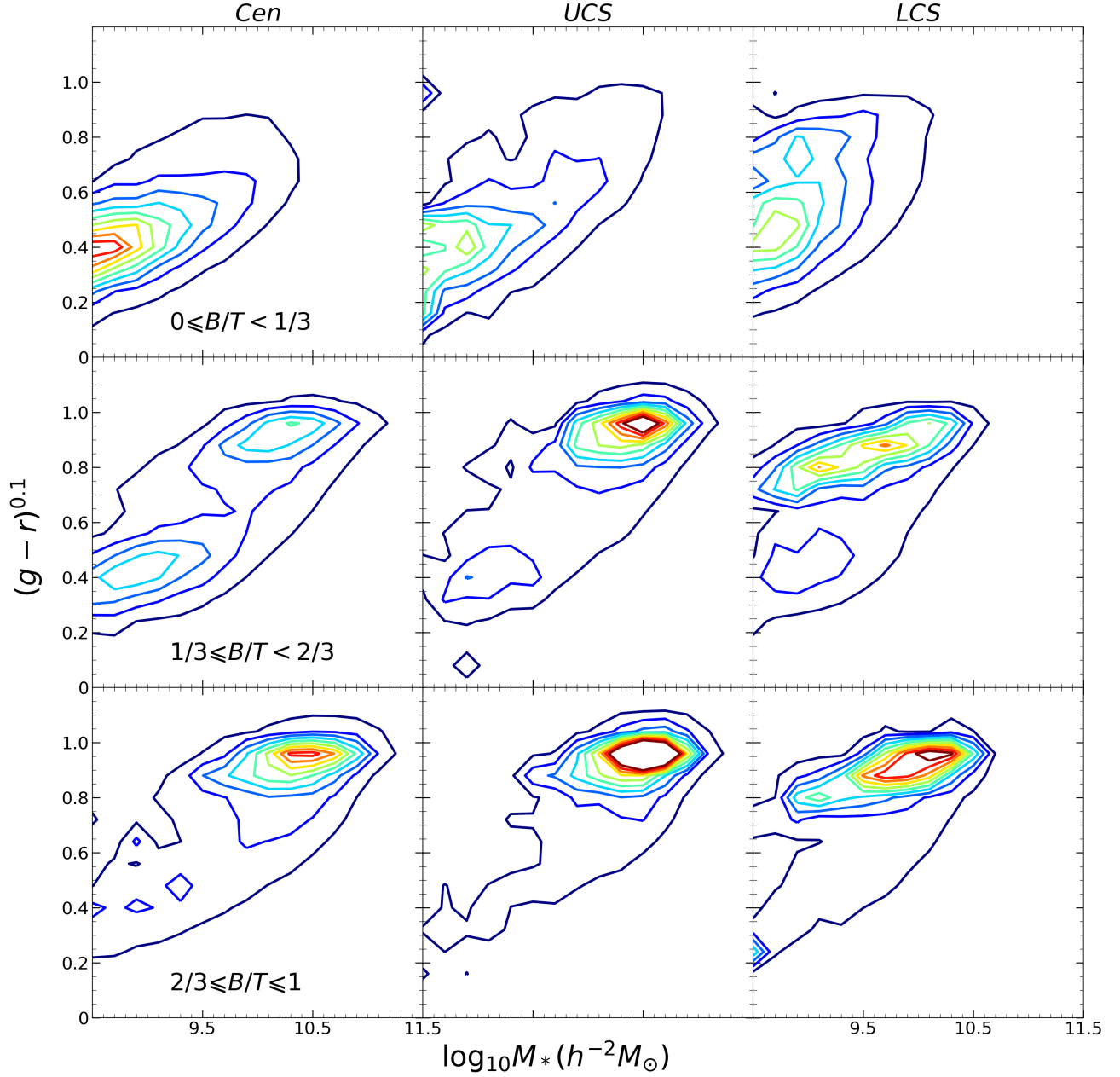


FIG. 3.— Similar to 2. Columns from left to right are the $(g - r)^{0.1}$ - M_* diagrams of Cen (central galaxies), UCS (upper class satellite galaxies) and LCS (lower class satellite galaxies). Rows from top to bottom correspond to different B/T bins: $0 \leq B/T < 1/3$, $1/3 \leq B/T < 2/3$, $2/3 \leq B/T \leq 1$.

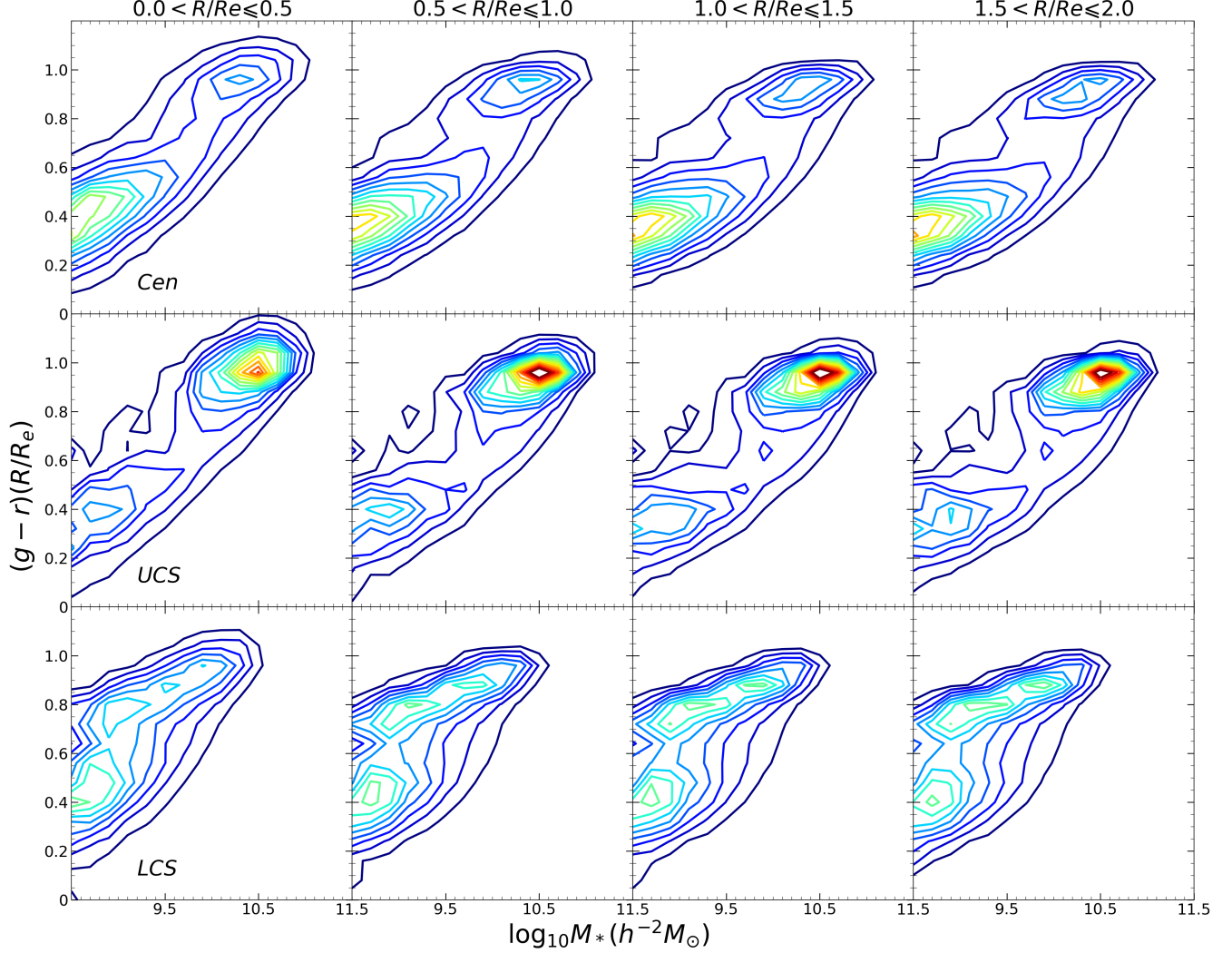


FIG. 4.— $(g - r)(R/R_e)$ - M_* diagrams. Rows from top to bottom are for Cen, UCS and LCS galaxies. Columns from left to right are $(g - r)(R/R_e)$ calculated in different annuli: $R/R_e \leq 0.5$, $0.5 < R/R_e \leq 1.0$, $1.0 < R/R_e \leq 1.5$ and $1.5 < R/R_e \leq 2.0$. We have each galaxy weighted here. For the lower-class galaxies, we can see clearly, there are two components for the quiescent galaxies. It is particularly significant at the outer region.

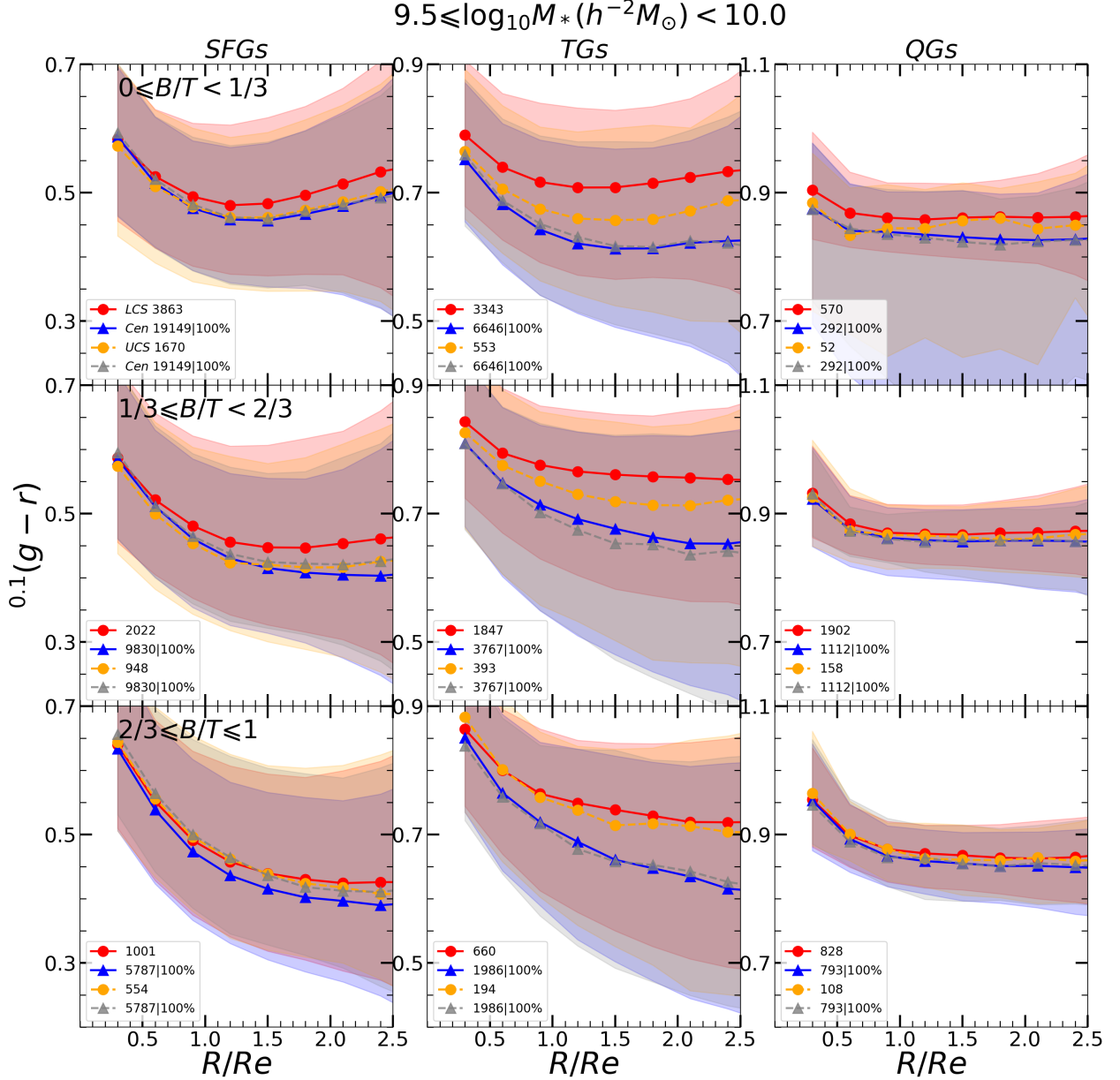


FIG. 5.— The median ($g - r$) as a function of R/R_e of galaxies of $9.5 \leq \log M_*/h^{-2}M_\odot < 10.0$. The results of central-lower class satellite pairs are shown in solid lines as indicated and that of the central-upper class satellite pairs are shown in dashed lines. The number of each type of galaxies together with the percent of the matched central galaxies is labeled. Three rows from top to bottom: $0 \leq B/T_m < 1/3$, $1/3 \leq B/T_m < 2/3$ and $2/3 \leq B/T_m \leq 1$. Three columns from left to right shows the results of blue clouds galaxies, green valley galaxies and red sequence galaxies. Error bars are with 1σ error. If a bin with galaxy number below 50, we ignore it. **here, perhaps, we should show the results for $9.0 \leq \log M_*/h^{-2}M_\odot < 9.5$**

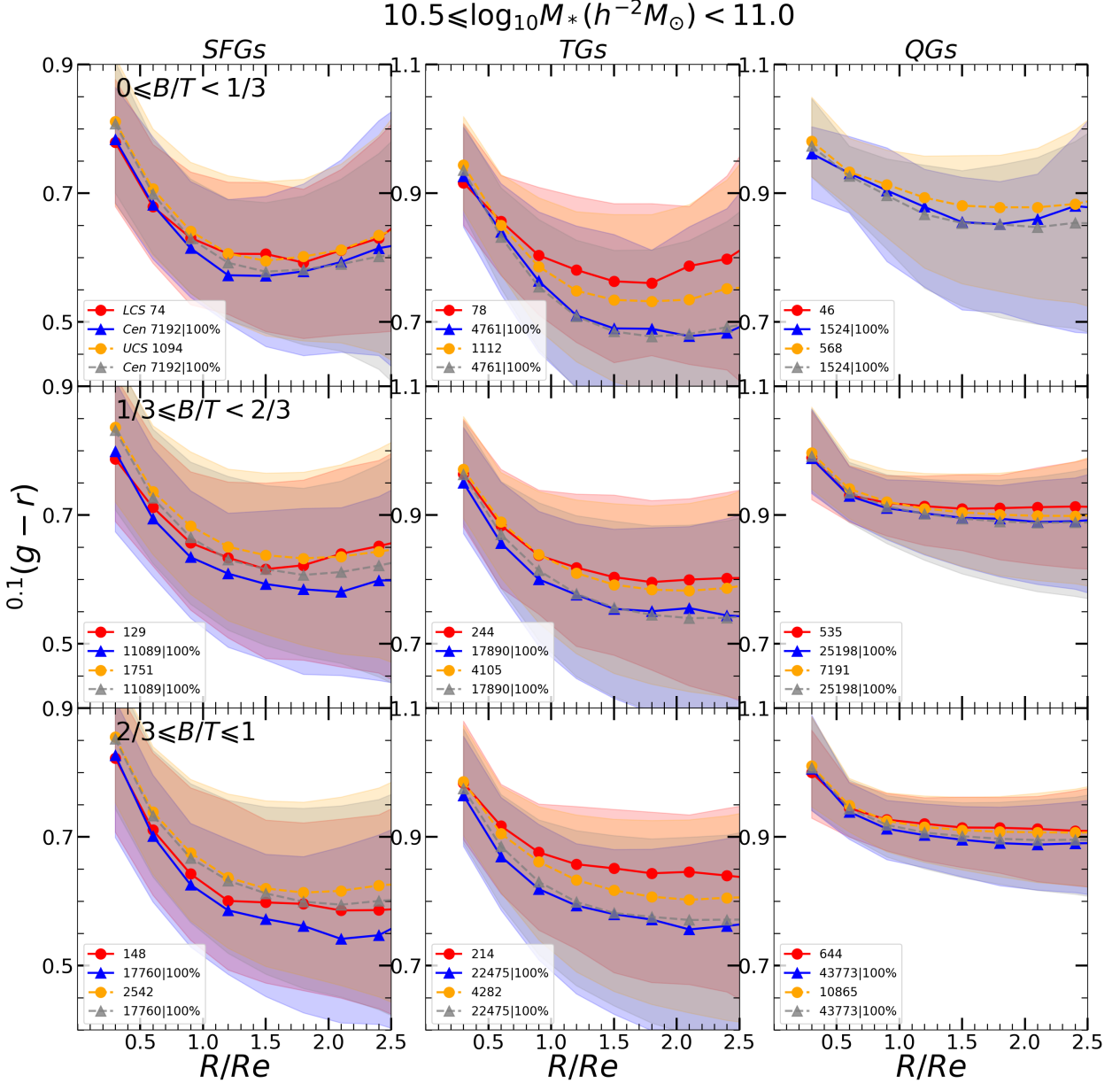


FIG. 6.— Similar to Figure 5, but for $10.5 \leq \log M_*/h^{-2} M_\odot < 11.0$

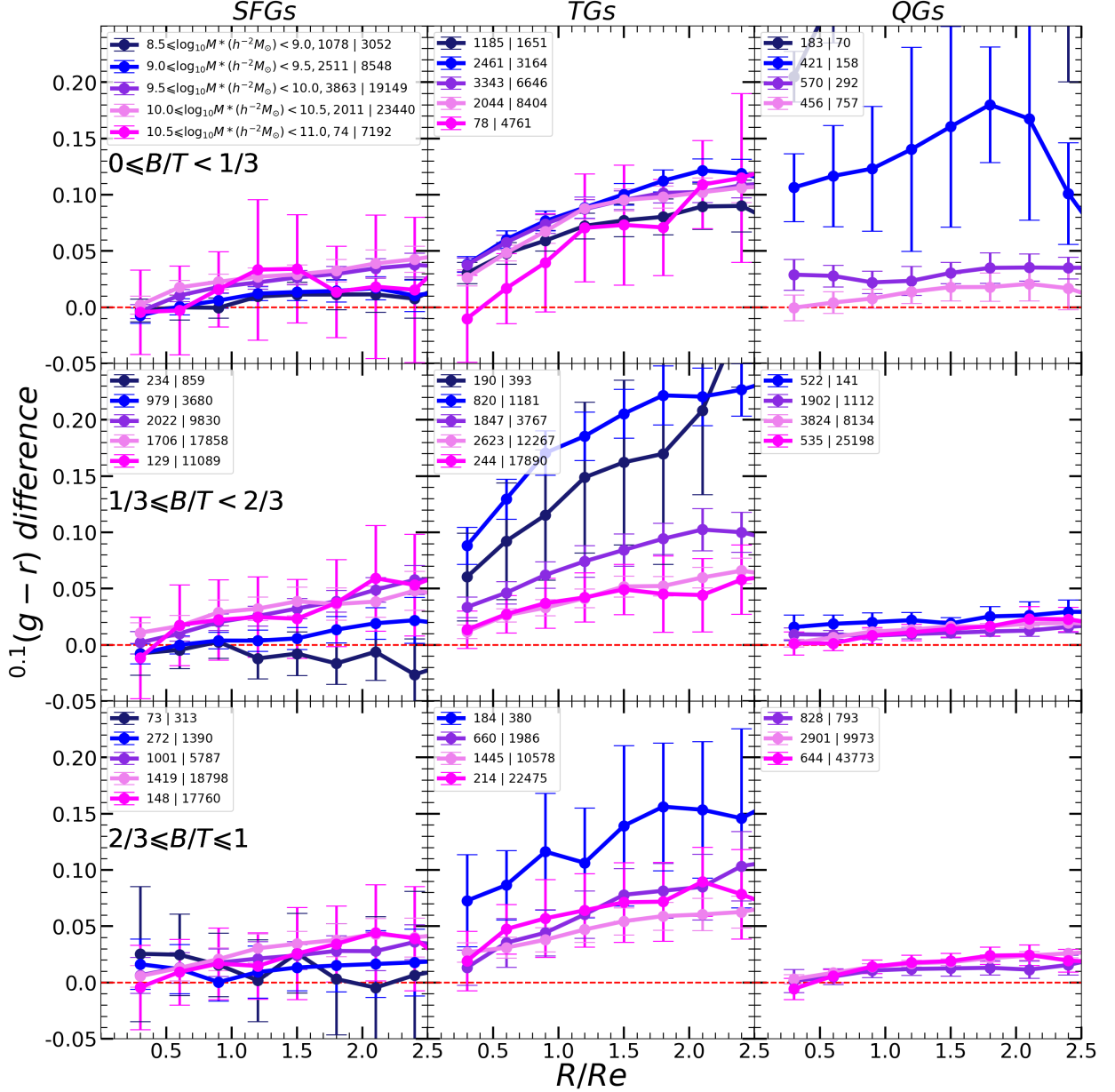


FIG. 7.— Color difference of central-lower class satellite pairs as function of R/R_e . Three rows are for $0 \leq B/T_m < 1/3$, $1/3 \leq B/T_m < 2/3$ and $2/3 \leq B/T_m \leq 1$. Three columns show the results of blue cloud galaxies, green valley galaxies and red sequence galaxies. In each panel, different colors correspond to the results of different M_* and the label shows the number of lower class satellite galaxies and central galaxies from left to right. We ignore the result of a bin if the number of lower class galaxies or central galaxies is below 50.

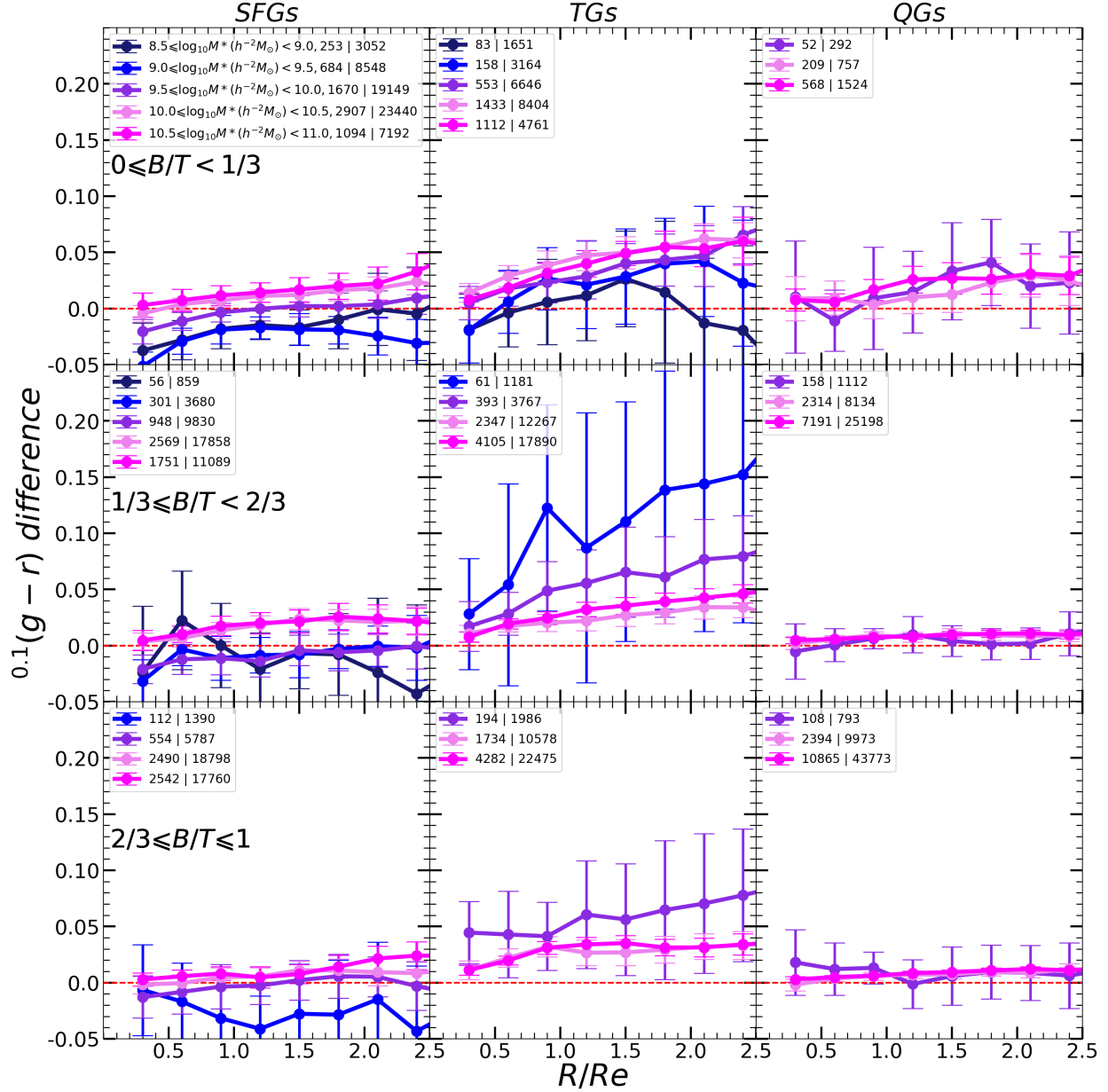


FIG. 8.— Similar to Figure 7, but for the central-upper class satellite pairs.

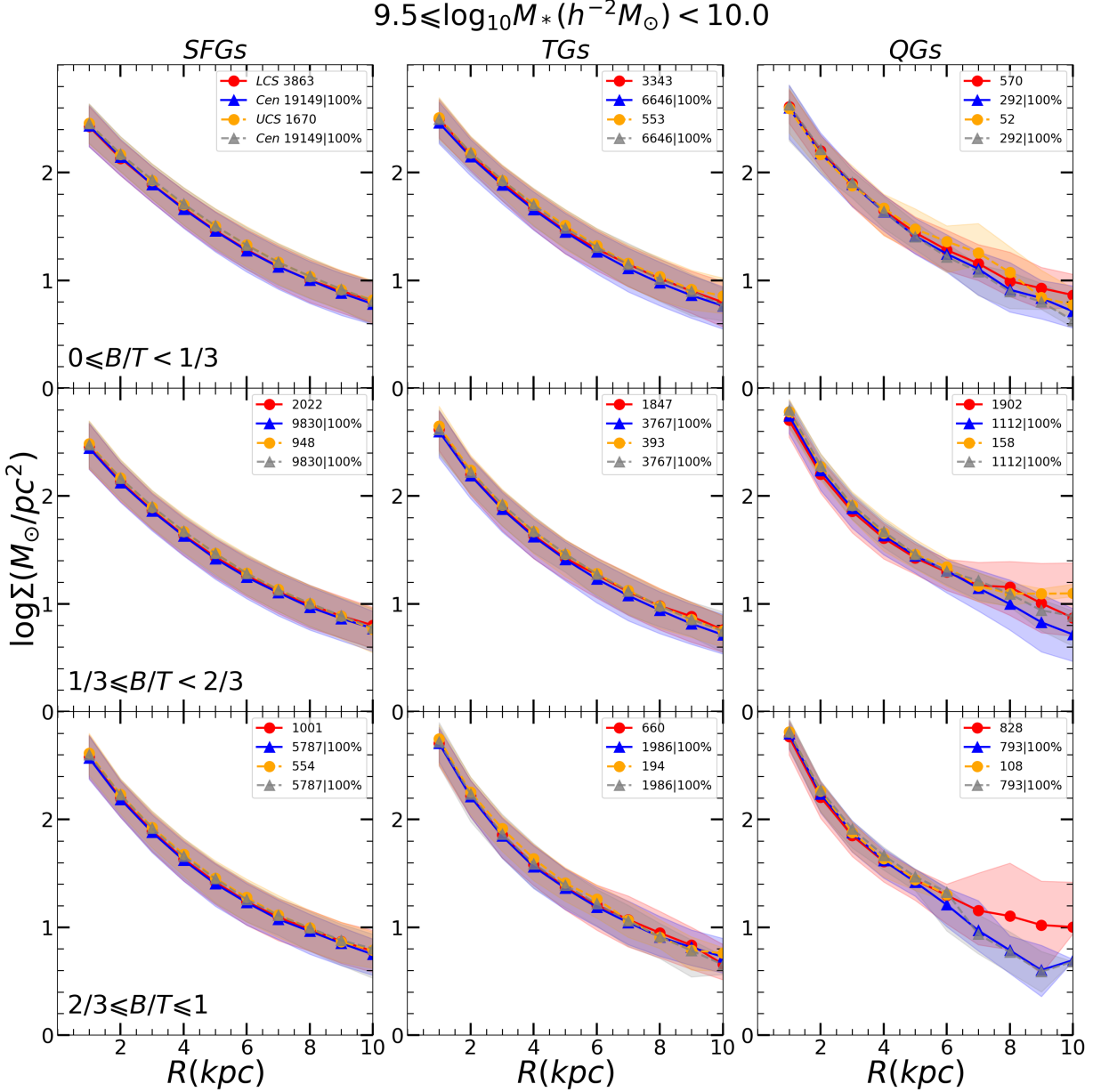


FIG. 9.— Similar to Figure 5, but for the surface mass density as a function of $R(kpc)$ of galaxies of $9.5 < \log M_*/h^{-1} M_\odot < 10.0$.

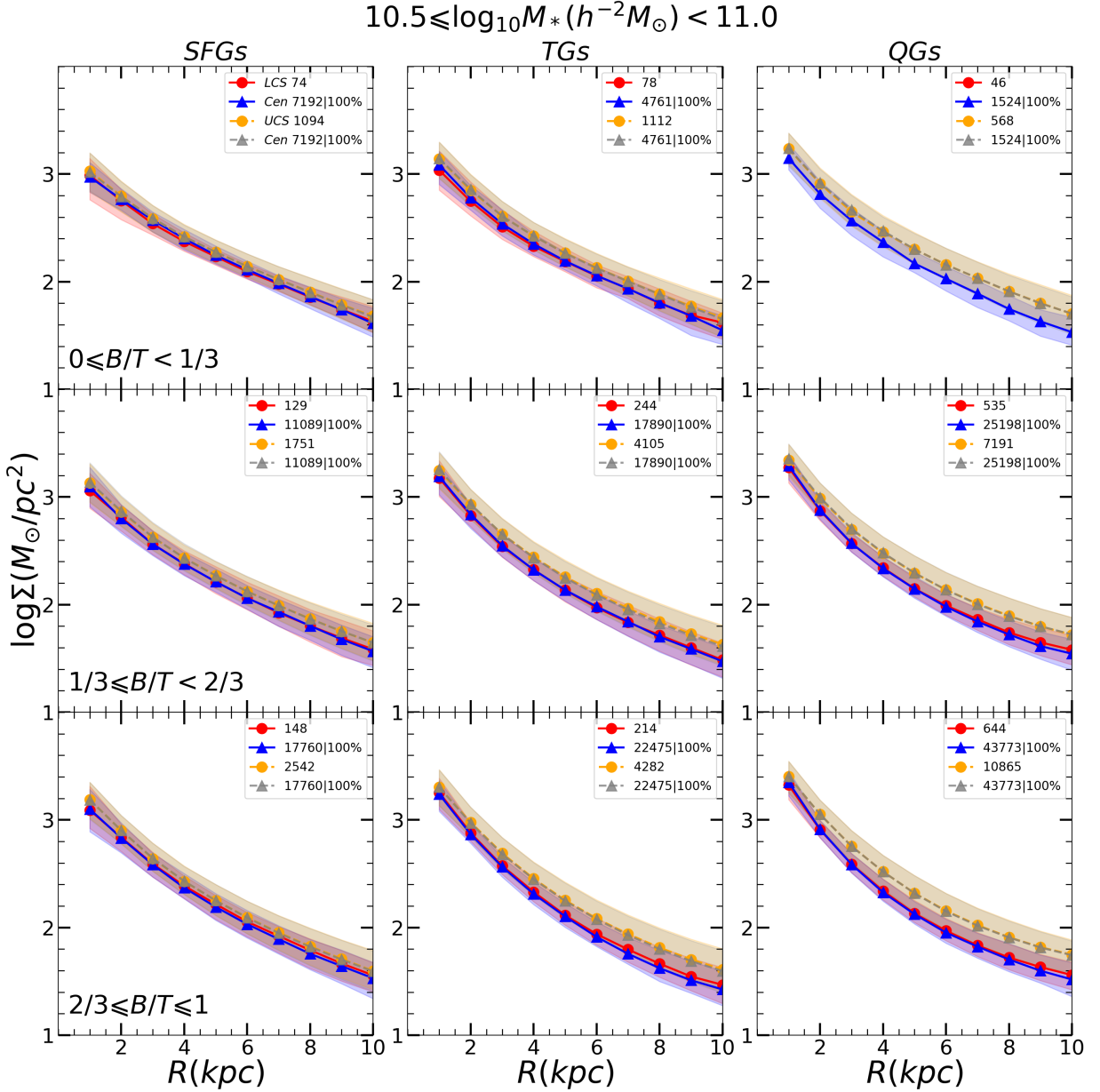


FIG. 10.— Similar to Figure 9, but for $10.5 < \log M_*/h^{-1} M_\odot < 11.0$.

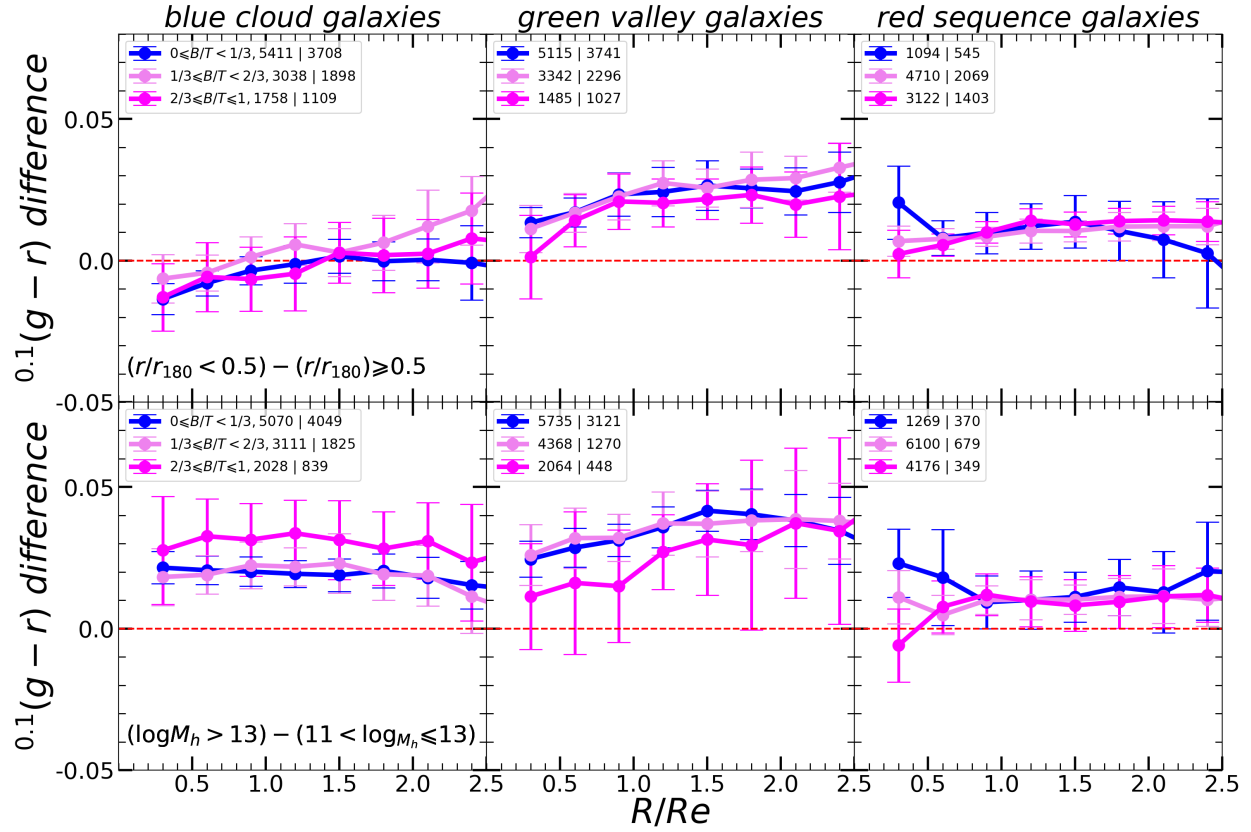


FIG. 11.—

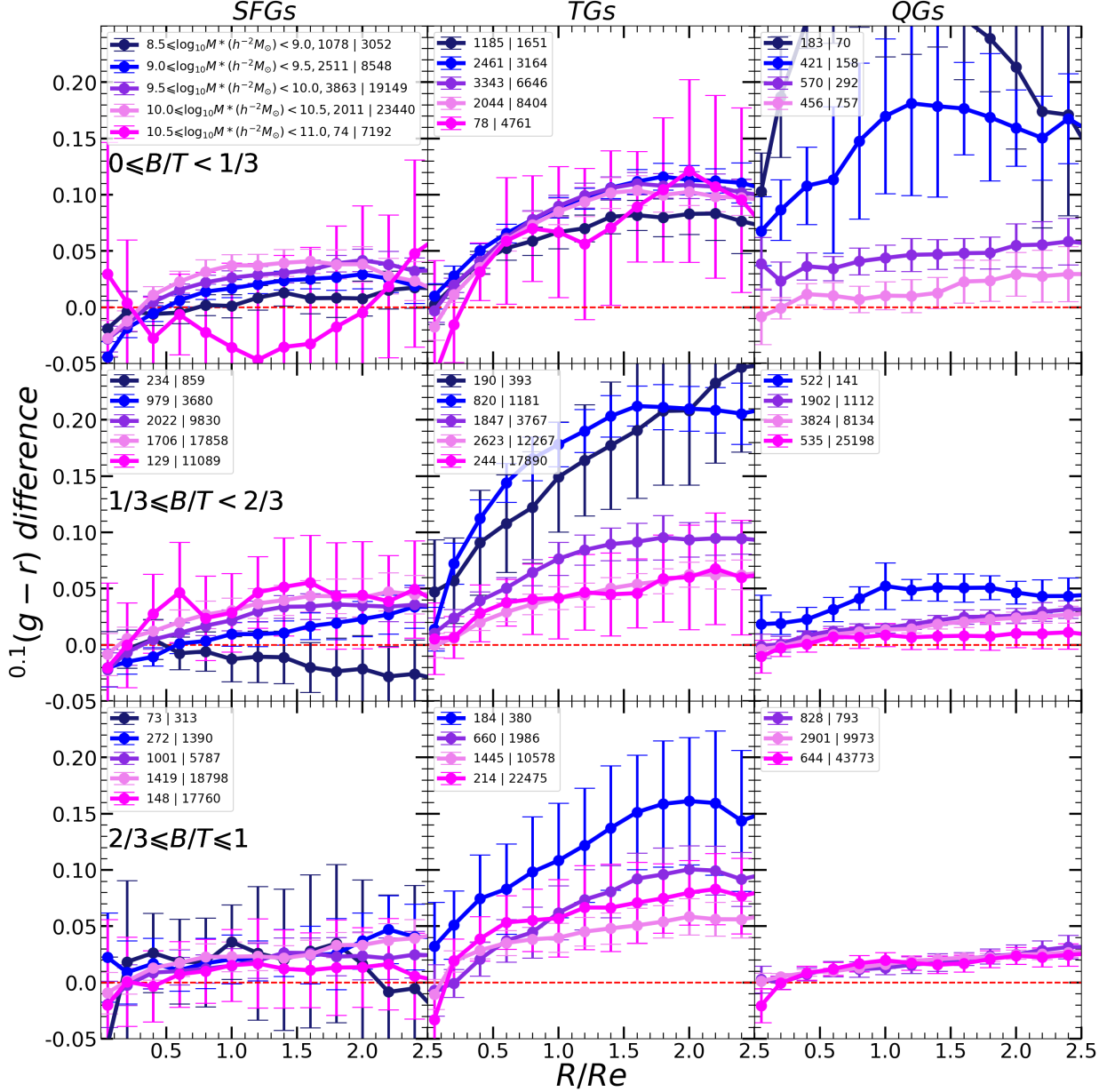


FIG. 12.— Similar to Figure 7, except that the $(g-r)$ is calculated using the Sersic fits profile.

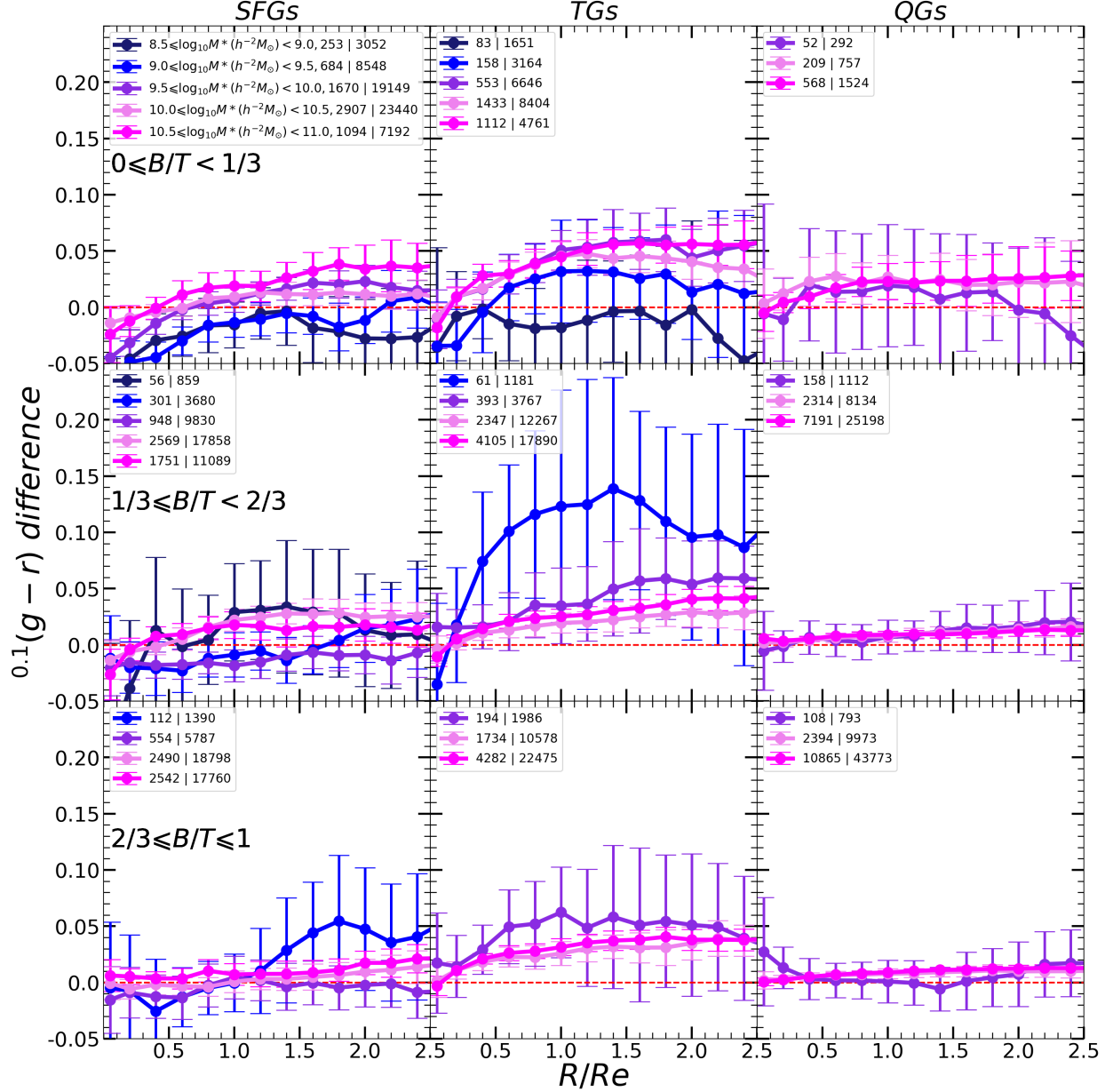


FIG. 13.— Similar to Figure 12 but for the central-upper class satellite pairs.